Electron Paramagnetic Resonance Studies of the Soluble Cu_A Protein from the Cytochrome ba_3 of *Thermus thermophilus*

Martin Karpefors,* Claire E. Slutter,§ James A. Fee,¶ Roland Aasa,* Bruno Källebring,* Sven Larsson,# and Tore Vänngård*

*Department of Biochemistry and Biophysics, Göteborg University and Chalmers University of Technology, Göteborg, Sweden; #Department of Physical Chemistry, Chalmers University of Technology, Göteborg, Sweden; §Division of Chemistry and Chemical Engineering, California Institute of Technology, Pasadena, California, USA; and ¶Department of Biology, University of California at San Diego, La Jolla, California, USA

ABSTRACT The electron paramagnetic resonance (EPR) spectrum of the binuclear Cu_A center in the water-soluble subunit II fragment from cytochrome ba_3 of *Thermus thermophilus* was recorded at 3.93, 9.45, and 34.03 GHz, and the EPR parameters were determined by computer simulations. The frequency and M_I dependence of the linewidth was discussed in terms of g strain superimposed on a correlation between the A and g values. The g values were found to be $g_x = 1.996$, $g_y = 2.011$, $g_z = 2.187$, and the two Cu ions contribute nearly equally to the hyperfine structure, with $|A_x| \approx 15$ G, $|A_y| = 29$ G, and $|A_z| = 28.5$ G (^{65}Cu). Theoretical CNDO/S calculations, based on the x-ray structure of the *Paracoccus denitrificans* enzyme, yield a singly occupied antibonding orbital in which each Cu is π^*-bonded to one S and σ^*-bonded to the other. In contrast to the equal spin distribution suggested by the EPR simulations, the calculated contributions from the Cu ions differ by a factor of 2. However, only small changes in the ligand geometry are needed to reproduce the experimental results.

INTRODUCTION

Nature relies on copper in the performance of a variety of oxidation-reduction processes. These include single electron transfer, dioxygen transport, oxygen activation, and multi-electron dioxygen reduction and are carried out by proteins that bind Cu and utilize its Cu(I) and Cu(II) valence states. The premier example of this has been the proteins with so-called blue sites, the properties of which have been the subject of intensive investigation for more than 30 years (cf. Adman, 1991; Solomon and Lowery, 1993; Malmström, 1994, for reviews). In these sites, the spectroscopic features of Cu(II) arise from an extensive mixing of the wave functions of the metal ion and a ligand sulfur.

Progress during the past few years has revealed the underlying chemistry behind an additional class of Cu sites, namely the so-called purple or Cu_A site. This was first recognized as such in N_2O reductase (N_2OR) (Kroneck et al., 1988), but these authors also predicted that the Cu_A site of cytochrome oxidase and the purple site of N_2OR were structurally related, if not identical. Three recent x-ray structures of Cu_A centers have vindicated this prediction (Iwata et al., 1995; Wilmanns et al., 1995; Tsukihara et al., 1995) (the x-ray structure of the Cu_A center of *Thermus thermophilus* has not yet been determined). Although higher resolution will be required to resolve some questions of detail, the present data show convincingly that the Cu_A center of the cytochrome c oxidases consists of a nominally planar ring formed by two Cu ions bridged by two RS^- groups of cysteines. In addition, each Cu is strongly coordinated to an imidazole ring of histidine and weakly to one additional atom, either the S of the conserved methionine or the carbonyl oxygen of a nearby peptide bond. The overall geometry may be viewed as distorted tetrahedral or as distorted trigonal, with the longer bond to the "extra" ligand atom being of questionable importance in determining the properties of the center.

As one of the canonical sites in cytochrome c oxidases, Cu_A has been widely studied since its discovery in 1962 (Beinert et al., 1962), and already in the 1960s the distinguishing features of the oxidized form of this center were recognized to be its intense long-wavelength absorption band (~800 nm), its small EPR g values of ~2.18 and ~2.00, and a small hyperfine interaction. Whereas the initial discussions of these properties focused on mononuclear models (see Malmström and Aasa, 1993), it is now possible to understand the properties of Cu_A in terms of a locus of two Cu ions.

Of interest here are the magnetic properties of the oxidized form. Recent EPR studies of the ba_3-Cu_A signal show that the signal originates from 2 Cu ($I = 3/2$ nuclei) and derives from an $S = 1/2$ spin system (Fee et al., 1995). In the present study the EPR parameters for the Cu_A center of *Thermus thermophilus* have been determined by simulation of spectra recorded at three different frequencies, taking M_I-dependent linewidth into account. The near equivalence between the two Cu atoms can be reproduced in molecular orbital calculations based on the structures published by Wilmanns et al. (1995) and Iwata et al. (1995), but in the

Received for publication 8 April 1996 and in final form 2 August 1996.

Address reprint requests to Dr. Martin Karpefors, Department of Biochemistry and Biophysics, Göteborg University and Chalmers University of Technology, Lundberg Laboratory, Medicinaregatan 9c, S-413 90, Göteborg, Sweden. Tel.: 46-31-773-3940; Fax: 46-31-773-3910; E-mail: martin.karpefors@bcbp.gu.se.

0006-3495/96/11/2823/07 $2.00

latter case only if slight changes are introduced into the published crystallographic structures.

MATERIALS AND METHODS

Sample preparation

The origin and properties of the isotopically enriched Cu_A samples were described previously (Fee et al., 1995), and the general properties of the soluble cytochrome ba_3-Cu_A protein from *T. thermophilus* have now been published (Slutter et al., 1996). Briefly, purified protein samples enriched with ^{63}Cu or ^{65}Cu were obtained by freeze-drying and redissolving the protein into water or 40% ethylene glycol to give a final buffer concentration of ~100 mM ammonium succinate at pH 4.6. The protein concentration was ~1.5 mM, as determined by double integration of the Cu EPR spectra. The samples were prepared in San Diego and shipped on dry ice to Göteborg for EPR measurements.

EPR spectroscopy

EPR spectra at 3.93 and 9.45 GHz were recorded at 20 K with a Bruker ER 200D-SRC spectrometer equipped with an Oxford Instruments ESR-9 helium flow cryostat. For 3.93 GHz spectra, an ER 061 SR microwave bridge, an ER 6102 SR reentrant cavity, and a homemade quartz insert were employed. Spectra at 34 GHz were recorded at 20 K with a Bruker ESP 380 spectrometer, using an ER 050 QG bridge and an ER 5103 QT cavity. Low temperatures were obtained with a Bruker Flexline ER 4118 CF helium cryostat. Quantifications of EPR spectra were performed under nonsaturating conditions as described earlier (Aasa and Vänngård, 1975), with Cu(II) in 2 M $NaClO_4$ (pH 2) as reference. EPR simulations were made with a homemade program, treating the hyperfine interaction by first-order perturbation theory and applying Gaussian lineshapes.

Theoretical methods

The calculations were based on the coordinates kindly provided by Dr. Hartmut Michel and Dr. Matti Saraste. The Cu_A center is in a mixed-valence Cu(II)–Cu(I) state formed by two Cu ions and the six residues His181, Cys216, Glu218, Cys220, His224, and Met227 (the residue numbering follows Michel's coordinate set from *Paracoccus denitrificans*). Cu(II) has nine 3d electrons, and thus one electron is missing from a closed shell, which means that the highest occupied molecular orbital is singly occupied (SOMO). Eight atoms form the inner core of the Cu_A center, which consists of two Cu ions, two Cys S, two His N, one Glu O, and one Met S. The S 3p orbitals from Cys216 and Cys220 and the Cu 3d orbitals are comparable in energy and, therefore, the largest contribution to SOMO is a strong antibonding interaction between the S 3p and the in-plane Cu 3d orbitals (see Fig. 4). The two N 2p orbitals from His181 and His224, together with a carbonyl O 2p orbital from a Glu218, have lower energies and form ligand bonds with the Cu ions. An additional S from a conserved Met227 also interacts weakly with the Cu_A center.

All calculations were carried out using the full coordinate set of 101 atoms and 299 electrons from the two Cu ions and the six liganding residues. The program used is a combination of CNDO/S and local density methods (Larsson et al., 1988), and these methods have been generalized to make the inclusion of heavy atoms possible. The atomic energy is $\alpha = (I + A)/2$, and the interelectronic repulsion energy is $\gamma = I - A$, where I is the ionization energy and A is the electron affinity. After the self-consistent field treatment, a configuration interaction calculation is performed, where double-projected singly substituted Slater determinants are included.

RESULTS

The water-soluble Cu_A fragment of subunit II from cytochrome ba_3 of *T. thermophilus* was labeled with ^{63}Cu and ^{65}Cu. Three different microwave frequencies were used: Q-, X-, and S-band at about 34, 9.5, and 4 GHz, respectively. The EPR spectra arise mainly from the Cu_A center, but quantitation showed that the ^{63}Cu-enriched sample contained 15% of a Type 2 Cu(II) signal, whereas the ^{65}Cu sample contained very little (<5%) extraneous signal. It was observed that the addition of ethylene glycol increased the resolution of the spectra substantially. For example, without this cryoprotectant the line at lowest field in the S-band spectrum was broadened almost beyond detection.

The ratio of the nuclear magnetic moment of ^{65}Cu to that of ^{63}Cu is 1.071, and because the hyperfine couplings are proportional to the moments they should appear with the same ratio. In an earlier publication (Fee et al., 1995) we found that the ratio of the hyperfine splittings is indeed close to 1.07. Furthermore, the observed splitting is dominated by interactions with Cu nuclei, and the Cu_A center is characterized by a binuclear mixed-valence Cu(1.5)–Cu(1.5) site sharing a single unpaired electron. Thus, most simulations were based on a model with the electronic spin $S = 1/2$ interacting with two equivalent $I = 3/2$ nuclei, dictating seven hyperfine lines with relative intensities 1:2:3:4:3:2:1. These can be labeled with $M_I = m_{I1} + m_{I2}$, which takes integer values from -3 to $+3$.

Because the ^{63}Cu sample was impaired by a larger extraneous signal, from here on ^{65}Cu will be considered in most figures and simulations. From the Q-band spectrum (Fig. 1), which revealed no observable hyperfine structure, the g_z value was determined to be 2.187, and the g values in the perpendicular region were close to 2. Experimental and

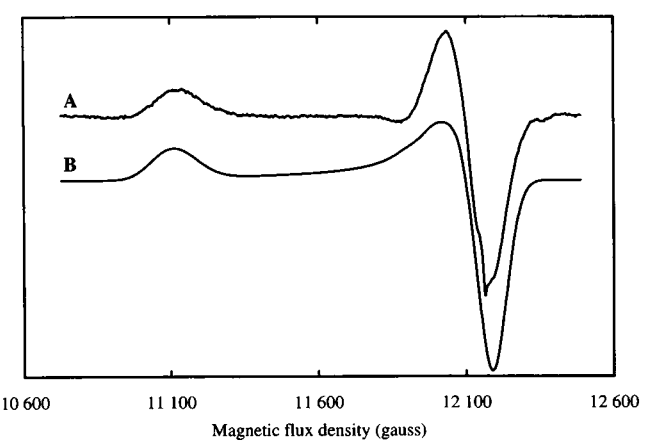

FIGURE 1 Experimental (*A*) and simulated (*B*) Q-band EPR spectra of the ^{65}Cu-enriched, water-soluble Cu_A-protein from the cytochrome ba_3 of *T. thermophilus*. The experimental spectrum was recorded with the following spectrometer settings: microwave frequency, 34.03 GHz; microwave power, 0.66 mW; modulation amplitude, 18 G; time constant, 82 ms; sweep time, 41 s; number of scans, 10. The protein concentration was 1.3 mM, and the samples in this and the following figures all contained 40% ethylene glycol. The simulated spectrum is a sum of 31 different simulated spectra (see text); parameters are given in Table 1. The narrow signal at $g = 2.00$ is due to a free-radical impurity, and the difference between the experimental and simulated spectra at around 11 850 G originates from Type 2 Cu(II) impurities.

simulated spectra at 34 GHz are shown in Fig. 1. The simulated spectrum with parameters according to Table 1 is derived from a summation procedure that will be explained below. On the low-field side of the perpendicular region one can see that even though the ^{65}Cu sample contains very little Type 2 Cu(II), this is still detectable.

As clearly seen in X- and S-band spectra (Figs. 2 and 3) and as already pointed out (Froncisz et al., 1979; Antholine et al., 1992), the hyperfine structure is much more prominent at lower microwave frequencies. This is due to the fact that all molecules in the sample are not identical, but will differ slightly in their g values. Therefore, there will be a larger spread of the lines at a higher frequency, and consequently the resolution will be higher at S- and X-bands than at the Q-band. In the S- and X-band spectra it is possible to discern part of the characteristic seven-line multiplet arising from the binuclear Cu site. The low-field side of the S-band spectrum shows the parallel hyperfine splittings, with the fourth line from the left situated at $g_z = 2.187$, in agreement with the Q-band result. The interpeak distance was measured by inspection to be 30 G. The splitting on the high field side was found to be 29 G and was interpreted as the high-field part of a seven-line structure centered on $g = 2.011$.

The g value of 2.011 and A value of 29 G were assigned to one of the axes only, and specifically to the y axis, because simulations in the X-band showed that the remaining undetermined g value was smaller than 2.011. To get consistency between the three different frequencies, g_x was chosen to be 1.996. No resolved feature could be associated with A_x, but simulations suggested that its value lies in the range of 10–20 G.

M_I dependence of the linewidth of the hyperfine lines

A straightforward simulation at 3.93 GHz based on the values given above, however, will not be in acceptable agreement with the experimental spectrum. This is illustrated by the simulated spectrum in Fig. 3 *D*, where the amplitude of the line at lowest field is far too high. Moreover, the resolved structure in the center of the simulated spectrum has no correspondence in the experimental spectrum. By permitting the linewidths to depend on M_I, we were able to obtain a better agreement between observed and calculated spectra and to determine the parameters more accurately.

An M_I dependence of the linewidth can be introduced into the simulations by allowing a spread in the g values, correlated to a variation in the A values (see, for example, Pilbrow, 1990). In the present work, a simple and straightforward approach is taken in the following manner. First, the field position, B', of the most narrow hyperfine line in the experimental spectrum with $M_I = M_I'$ was noted. Then a

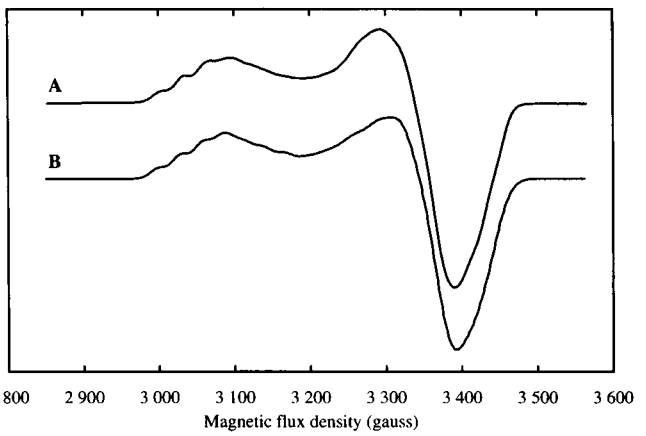

FIGURE 2 X-band EPR spectra, experimental (*A*) and simulated (*B*), of the ^{65}Cu-enriched, water-soluble Cu_A-protein from the cytochrome ba_3 of *T. thermophilus*. Spectrometer settings: microwave frequency, 9.45 GHz; microwave power, 0.2 mW; modulation amplitude, 10 G; time constant, 200 ms; sweep time, 200 s; number of scans, 1. The protein concentration was 1.3 mM. Simulation as in Fig. 1 (see Table 1).

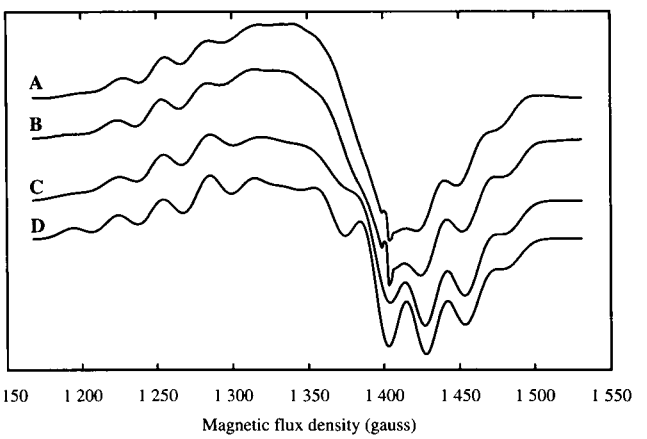

FIGURE 3 Experimental S-band EPR spectra, of the ^{63}Cu-enriched (*A*) and ^{65}Cu-enriched (*B*), water-soluble Cu_A-protein from the cytochrome ba_3 of *T. thermophilus*. Spectrometer settings: microwave frequency, 3.93 GHz; microwave power, 2.0 mW; modulation amplitude, 6.3 G; time constant, 100 ms; sweep time, 100 s; number of scans, 32. The protein concentration was 1.3 mM. The lower spectra are simulations of the ^{65}Cu-protein, where *C* is a summed spectrum as in Fig. 1 and *D* is a spectrum without a g-A correlated variation. The narrow signal at $g = 2.00$ in the experimental spectra is due to the same free-radical impurity as seen in Fig. 1.

TABLE 1 Parameters used for the EPR simulations

	x	*y*	*z*
g	1.996	2.011	2.187
Distribution width*		± 0.012	± 0.011
|*A*| (G)#	15	29	28.5
Distribution width (*G*)*		± 3.3	± 6.5
Linewidths (G)			
S-band	20	18	17
X-band	25	31	22
Q-band	90	70	90

*The values indicate the (half-height) width of the g-A correlated distribution used in the simulations.
#^{65}Cu.

number of component spectra were simulated with this hyperfine line remaining at B'. This imposes a relation between the component g and A values, and differentiation of this relation shows that the parameters of the component spectra should be taken around the central values such that $\Delta A/\Delta g = -h\nu/g^2\beta M_I'$, where ν is the microwave frequency, h is Planck's constant, and β is the Bohr magneton. Before the component spectra were summed, they were weighted according to a discrete Gaussian distribution. The width of the distribution was chosen so that the outermost spectra contributed around 3% compared to the middle spectrum, and a sufficient number of spectra were included to get a smoothed Gaussian lineshape in the summed spectrum.

In the S-band, at the parallel region, the third line from the left (that is the $M_I = -1$ line, assuming $A < 0$; Vänngård, 1972) is narrowest. A total of 31 component spectra were summed, with their $|A_z|$ values varying in 1 G steps. The corresponding g values were chosen so that $|\Delta A_z|/\Delta g_z$ was -570 G; the optimal average g_z and A_z values are given in Table 1. Note that the A_z value differs significantly from the one obtained by inspection of the experimental spectrum. For the y direction, $|A_y|$ was varied around 29 G in steps of 0.5 G, and B' was measured at a position between the first and second lines from the right, because these lines were equally narrow. This yields $|\Delta A_y|/\Delta g_y = 290$ G. A similar distribution of values of A_x did not improve the fit with the experimental spectrum, so it was left constant at 15 G. The deviation of the simulated from the experimental S-band spectrum in the middle region coincides, in g value terms, with the deviation in the Q-band at the low-field part of the perpendicular region, which indicates that these deviations could be due to a contaminating paramagnetic species.

The g and A values derived for the 31 components representing the S-band spectrum were then used for X-band simulations. Fig. 2 shows the resulting spectrum after the summation procedure, together with the experimental spectrum. As a consequence of the higher frequency, and in agreement with the experimental spectrum, the narrowest line in the z direction turns out to be the $M_I = -2$ line. Because of M_I- and frequency-dependent linewidth, the hyperfine structure on the high-field side of the parallel region is not resolved.

Identity of the two copper ions

In the simulations described above it was assumed that the two copper ions had identical EPR parameters. Separate simulations of the S-band spectrum (not shown) indicated that their hyperfine coupling constants can differ by at most 8 G in both the y and z directions, i. e., the difference between the two ions is less than 25%. This conclusion is consistent with Cu-ENDOR spectra (P. Doan and B. Hoffman, unpublished observations).

DISCUSSION

Quadrupole interactions

Possible influences of quadrupole interactions from the Cu nuclei are not included in our simulations. These can, in principle, give displacements of the allowed hyperfine lines ($\Delta m_I = 0$) and create forbidden transitions ($\Delta m_I = \pm 1, \pm 2$) between the allowed ones. In an ENDOR study (Gurbiel et al., 1993) the Cu quadrupole coupling energy was found to be about 4 MHz, corresponding to 1.4 G. Using this figure we can estimate that the maximum shift in any allowed hyperfine line is less than 0.5 G, and the intensity of any forbidden transition is always less than 7% of the allowed transitions. Furthermore, both effects are much smaller in the low-field region (near g_z) of the spectrum (Abragam and Bleaney, 1970). Thus we can conclude that quadrupole interactions need not be considered in the simulations.

Linewidths

Part of the linewidth in the present spectra arises from a distribution of g and A values, and the M_I dependence is caused by a correlation between the two parameters. For the z direction most copper complexes have EPR spectra with the sharpest hyperfine line to the low-field side of g_z. This means that the magnitude of the hyperfine coupling increases as the g value decreases, i.e., $|\Delta A_z|/\Delta g_z$ is negative. The same sign is normally observed if one compares different Cu proteins belonging to the same class such as Type 1—a protein with a larger g_z has a smaller $|A_z|$. By comparison with theoretical expressions for the EPR parameters (see, for example, Gewirth et al., 1987, equation 19), such results are most easily explained under the assumption that A_z is negative, which then would be the case for the Cu_A complex. An inspection of the expression for the hyperfine constants, combined with our finding that for the y direction the sharpest line is at the high-field side, suggests, on the other hand, that A_y is positive. Using these signs, the observed values of $|\Delta A_y|/\Delta g_y$ and $|\Delta A_z|/\Delta g_z$ are consistent with the relations derived for the EPR parameters of mononuclear Cu complexes (Gewirth et al., 1987).

The linewidths of the components used in the simulations (Table 1) represent a broadening that does not originate in a strict g-A correlation. This width increases roughly linearly with the microwave frequency, which suggests that there is a substantial g-value strain not correlated with the hyperfine coupling. Extrapolation to zero microwave frequency yields a residual linewidth of approximately 10 G. A large fraction of this is due to unresolved ligand hyperfine coupling (Gurbiel et al., 1993), which from simulations using the known couplings from ENDOR are estimated to contribute 8–9 G. The remaining width is consequently quite small, which is consistent with the width observed in ENDOR, which amounts to 0.4 G.

Electronic structure

The EPR spectra recorded at the three microwave frequencies in this work can be simulated accurately with the same hyperfine tensors for the two copper ions with respect to both the principal elements and the directions of the principal axes. This suggests not only that the unpaired electron is equally distributed over the two metal ions, as discussed earlier, but also that the environment around each ion is symmetry-related. Indeed, in both the *Paracoccus denitrificans* protein (Iwata et al., 1995) and the engineered quinol oxidase from *Escherichia coli* (Wilmanns et al., 1995), the copper ions and the two bridging sulfur atoms form a symmetrical unit with all atoms approximately in the same plane.

The results of our calculations, presented in Table 2, show that the wave function of the unpaired electron is mainly determined by the strong interaction among these four atoms and is localized in this plane. For example, for the structure reported by Iwata et al. (1995), the Cu(II) $d_{x^2-y^2}$ and d_{xy} orbitals together account for 83% of the total copper contribution to SOMO. In Fig. 4 the atomic wave functions that dominate the SOMO in the Cu-S plane are illustrated as a contour plot, from which the antibonding character of the molecular orbital clearly appears. The p orbital on each sulfur forms a σ^* bond with the d orbital of one copper ion and a π^* bond with the other ion. The orientation of the cysteine side chain relative to the copper-sulfur moiety determines the orientation of the sulfur p orbital and thereby the character of each Cu-S bond. Although Table 2 shows that the ratio of the coefficients of $d_{x^2-y^2}$ and d_{xy} orbitals in the quinol oxidase structure is quite different from that in the *Paracoccus* protein, the same general bonding situation exists in the two cases. The π^* bond is related to the Cu-S bond in the blue copper proteins, whereas the σ^* bond is similar to the bond in the mutant of superoxide dismutase, where Cu coordinates three His and one Cys (Lu et al., 1992). The consequences of this arrangement for the optical spectrum will be discussed in a forthcoming publication.

From this wave function it is predicted that the z axis of both the g and the two A tensors is perpendicular to the plane, and that the x and y axes lie in the plane. However, in the case of *P. denitrificans* the calculations yielded al-

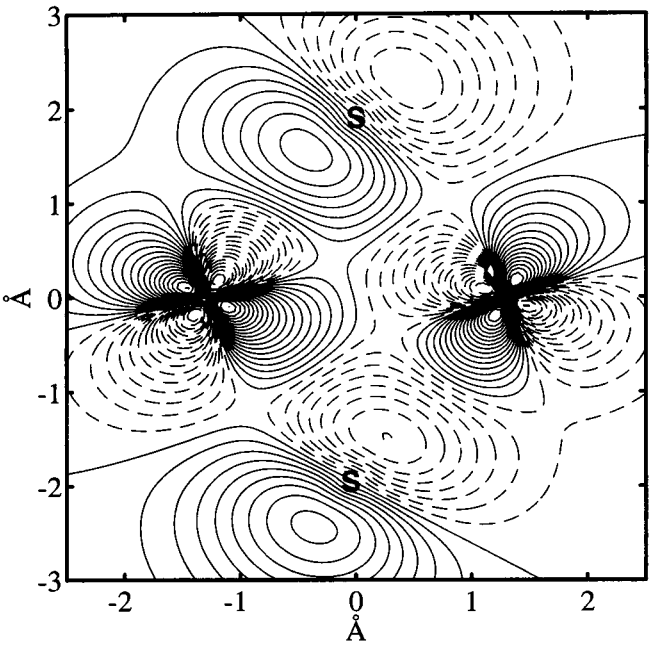

Figure 4 A Two-dimensional contour plot that illustrates the results from linear combination of atomic orbitals calculations on the unmodified Cu_A site from *Paracoccus denitrificans*, taking 101 atoms into account. The figure shows a superposition of the in-plane components of the Cu and S wavefunctions in the highest occupied molecular orbital. The solid and dashed lines represent part of the function with different signs. Each sulfur atom forms an antibonding π^* bond with one copper ion and an antibonding σ^* bond with the other ion.

most a 1:2 ratio for the density of unpaired electrons in the Cu(II) in-plane d orbitals at the two copper ions (Table 2, a). The copper hyperfine interaction in the EPR of the *Thermus* protein, which from the discussion above appears highly anisotropic and therefore to a major part must arise from unpaired electrons in metal d orbitals, indicates instead a 1:1 ratio. The great similarity between the *Thermus* and *Paracoccus* EPR spectra suggests that the same ratio applies to both proteins.

The predicted asymmetry in the distribution of the unpaired electron is, of course, caused by the asymmetry in the coordinates of the paramagnetic center. Therefore, calculations using various geometries were made. They showed

TABLE 2 Spin density distribution (%) from CNDO/S calculations on the Cu_A center for different configurations

	Cu1*				Cu2*				S Cys216*	S Cys220*	N His181*		N His224*	
Configuration	p	$d^{\#}$	$d_{x^2-y^2}$	d_{xy}	p	$d^{\#}$	$d_{x^2-y^2}$	d_{xy}	p	p	s	p	s	p
a. *Paracoccus*[§]	2.5	23.8	5.7	16.2	1.4	13.5	5.0	7.9	19.6	23.1	1.5	3.1	0.2	0.5
b. D_{2h} symmetry[¶]	2.5	24.0	6.2	15.5	1.4	13.8	5.8	7.4	19.1	22.8	1.6	3.3	0.3	0.7
c. Cys216 rotation	1.6	24.3	10.6	11.9	1.2	17.4	12.8	4.0	17.3	22.7	1.6	3.2	0.6	1.4
d. His181 rotation	2.2	22.2	10.6	10.5	1.4	16.7	7.9	7.9	22.2	21.4	0.7	1.6	0.3	0.8
e. Quinol oxidase[‖]	1.4	22.2	16.6	3.7	0.9	18.5	16.6	0.7	16.1	24.3	0.8	1.8	0.9	1.9

*The numbering of Iwata et al. is used.

#Includes contributions from all five d orbitals.

§Iwata et al. (1995).

¶The D_{2h} symmetry only refers to the Cu_2S_2 structure itself.

‖Wilmanns et al. (1995).

that the deviation from D_{2h} of the Cu_2S_2 structure itself, suggested by the crystallographic data, is not sufficient to cause the asymmetry (Table 2, b). Likewise, the measured differences in the distances to the other copper ligands are not the determining factor (not shown in Table 2). Rather, the major source of the asymmetrical unpaired electron density lies in the positions of the cysteine β-carbons and the histidine nitrogens relative to the Cu_2S_2 unit. For example, we found that it is sufficient to rotate the S-C_β bonds of Cys216 or His181 by 20° to reduce the difference between the unpaired electron densities on the two copper ions to nearly 25% (Table 2, c and d), i.e., close to the error limits of the experimental EPR spectra described above. Other changes in geometry could also reduce the electronic asymmetry; the modifications can be accommodated within the relatively large uncertainties of the present structure determination.

Despite the higher symmetry obtained through these geometrical adjustments (Table 2, c and d), the difference in the distribution of the unpaired electron between the two nitrogen ligands is not eliminated for the *Paracoccus* structure. The ratio of the spin densitites is calculated to be 2. This ratio is consistent with the ENDOR measurements showing a ratio of the couplings of 1.5 to 2 for the *Thermus* ba_3 protein (Gurbiel et al., 1993). Notably, it is the nitrogen in His181, which is most remote from copper, that is predicted to have the highest spin density, presumably because the orientation of the corresponding histidine plane is favorable for spin delocalization.

Using the coordinates from the purple CyoA protein, the ratio between the spin densities on the two copper ions was calculated to be much closer to 1, reflecting the higher symmetry, especially in the histidine ligands (Table 2, e). The remaining disproportion could be canceled by a small rotation of one of the cysteines. As expected, the distribution of the unpaired electron over the two nitrogen ligands was almost equal.

An interesting feature in the Cu_A EPR spectrum is the low values for g_x and g_y, which were observed very early (Beinert et al., 1962; Aasa et al., 1976). One g value appears to be less than 2.00, which seems to be difficult to explain by the classical treatment of copper complexes. The reason for these low g values is probably negative contributions from the sulfur ligands through spin-orbit coupling. Theoretical calculations of sulfur-liganded copper complexes have indeed indicated such effects (Keijzers and de Boer, 1975). Quantitatively, however, the contributions are too small, so a fuller understanding must await more extended calculations on the Cu_A center.

We thank Ms. Donita Sanders for assistance in preparing the ba_3-Cu_A samples, Drs. Hartmut Michel and Matti Saraste for sharing the crystallographic coordinates with us, Dr. Örjan Hansson for providing the original EPR simulation program, and Dr. John Pilbrow for useful comments.

The work was supported by National Institutes of Health grants GM 35342 (JAF) and GM 16424 (John H. Richards, Division of Chemistry and Chemical Engineering, California Institute of Technology, Pasadena, California, USA), a predoctoral training grant GM 07616 (CES), and grants from the Swedish Natural Science Research Council (TV, RA).

REFERENCES

Aasa, R., S. P. J. Albracht, K.-E. Falk, B. Lanne, and T. Vänngård. 1976. EPR signals from cytochrome *c* oxidase. *Biochim. Biophys. Acta.* 422: 260–272.

Aasa, R., and T. Vänngård. 1975. EPR signal intensity and powder shapes: a reexamination. *J. Magn. Res.* 19:308–315.

Abragam, A., and B. Bleaney. 1970. Electron Paramagnetic Resonance of Transition Ions. Clarendon Press, Oxford. 181–191.

Adman, E. T. 1991. Copper protein structure. *Adv. Protein Chem.* 42: 145–197.

Antholine, W. E., D. H. W. Kastrau, G. C. M. Steffens, G. Buse, W. G. Zumft, and P. M. H. Kroneck. 1992. A comparative EPR investigation of the multicopper proteins nitrous-oxide reductase and cytochrome c oxidase. *Eur. J. Biochem.* 209:875–891.

Beinert, H., D. E. Griffiths, D. C. Wharton, and R. H. Sands. 1962. Properties of the copper associated with cytochrome oxidase as studied by paramagnetic resonance spectroscopy. *J. Biol. Chem.* 237: 2337–2346.

Boça, R. 1987. Inclusion of relativistic effects into ZDO methods. 1. A quasi-relativistic CNDO/1. *Int. J. Quant. Chem.* 31:941–950.

Broo, A., and S. Larsson. 1992. *Ab initio* and semiempirical studies of electron-transfer and spectra of binuclear complexes with organic bridges. *Chem. Phys.* 161:363–378.

Fee, J. A., D. Sanders, C. E. Slutter, P. E. Doan, R. Aasa, M. Karpefors, and T. Vänngård. 1995. Multi-frequency EPR evidence for a binuclear Cu_A center in cytochrome *c* oxidase: studies with a ^{63}Cu- and ^{65}Cu-enriched, soluble domain of the cytochrome ba_3 subunit II from *Thermus thermophilus*. *Biochem. Biophys. Res. Commun.* 212:77–83.

Froncisz, W., C. P. Scholes, J. S. Hyde, Y.-H. Wei, T. E. King, R. W. Shaw, and H. Beinert. 1979. Hyperfine structure resolved by 2 to 4 GHz EPR of cytochrome c oxidase. *J. Biol. Chem.* 254:7482–7484.

Gewirth, A. A., S. L. Cohen, H. J. Schugar, and E. I. Solomon. 1987. Spectroscopic and theoretical studies of the unusual EPR parameters of distorted tetrahedral cupric sites: correlations to x-ray spectral features of core levels. *Inorg. Chem.* 26:1133–1146.

Gurbiel, R. J., Y.-C. Fann, K. K. Surerus, M. M. Werst, S. M. Musser, P. E. Doan, S. I. Chan, J. A. Fee, and B. M. Hoffman. 1993. Detection of two histidyl ligands by 35-GHz ENDOR: ^{14,15}N and ^{63,65}Cu ENDOR studies of the Cu_A site in bovine heart cytochrome aa_3 and cytochromes caa_3 and ba_3 from *Thermus thermophilus*. *J. Am. Chem. Soc.* 115: 10888–10894.

Iwata, S., C. Ostermeier, B. Ludwig, and H. Michel. 1995. Structure at 2.8 Å resolution of cytochrome *c* oxidase from *Paracoccus denitrificans*. *Nature.* 376:660–669.

Keijzers, C. P., and E. de Boer. 1975. E. S. R. study of copper and silver *N,N*-dialkyldiselenocarbamates. Part II. Interpretation of spectra measured in host lattices with monomeric structures. *Mol. Phys.* 29: 1007–1020.

Kroneck, P. M. H., W. E. Antholine, J. Rister, and W. G. Zumft. 1988. The cupric site in nitrous oxide reductase contains a mixed-valence [Cu(II),Cu(I)] binuclear center: a multifrequency electron paramagnetic resonance investigation. *FEBS Lett.* 242:70–74.

Larsson, S., A. Broo, B. Källebring, and A. Volosov. 1988. Long distance electron transfer. *Int. J. Quant. Chem. QBS.* 15:1–22.

Lu, Y., E. B. Gralla, J. A. Roe, and J. S. Valentine. 1992. Redesign of a type 2 into a type 1 copper protein: construction and characterization of yeast copper-zinc superoxide dismutase mutants. *J. Am. Chem. Soc.* 114:3560–3562.

Malmström, B. G. 1994. Rack-induced bonding in blue-copper proteins. *Eur. J. Biochem.* 223:711–718.

Malmström, B. G., and R. Aasa. 1993. The nature of the Cu_A center in cytochrome *c* oxidase. *FEBS Lett.* 325:1–2.

Pilbrow, J. R. 1990. Transition Ion Electron Paramagnetic Resonance. Clarendon Press, Oxford.

Slutter, C. E., D. Sanders, P. Wittung, B. G. Malmström, R. Aasa, J. H. Richards, H. B. Gray, and J. A. Fee. 1996. A water-soluble, recombinant protein domain of the cytochrome ba_3 subunit II from *Thermus thermophilus*. *Biochemistry*. 35:3387–3395.

Solomon, E. I., and M. D. Lowery. 1993. Electronic structure contributions to function in bioinorganic chemistry. *Science*. 259:1575–1581.

Tsukihara, T., H. Aoyama, E. Yamashita, T. Tomizaki, H. Yamaguchi, K. Shinzawa-Itoh, R. Nakashima, R. Yaono, and S. Yoshikawa. 1995. Structures of metal sites of oxidized bovine heart cytochrome c oxidase at 2.8 Å. *Science*. 269:1069–1074.

Vänngård, T. 1972. Copper proteins. *In* Biological Applications of Electron Spin Resonance. H. M. Swartz, J. R. Bolton, and D. C. Borg, editors. John Wiley and Sons, New York. 411–447.

Wilmanns, M., P. Lappalainen, M. Kelly, E. Sauer-Eriksson, and M. Saraste, 1995. Crystal structure of the membrane-exposed domain from a respiratory quinol oxidase complex with an engineered dinuclear copper center. *Proc. Natl. Acad. Sci. USA*. 92:11955–11959.